Materials and Design 54 (2014) 212–221

Contents lists available at ScienceDirect

Materials and Design

journal homepage: www.elsevier.com/locate/matdes

Effect of substrate surface roughening and cold spray coating on the fatigue life of AA2024 specimens

C.W. Ziemian [a,*], M.M. Sharma [a], B.D. Bouffard [b], T. Nissley [c], T.J. Eden [d]

[a] Bucknell University, Department of Mechanical Engineering, Lewisburg, PA 17837, USA
[b] Naval Surface Warfare Center, Carderock Division, West Bethesda, MD 20817, USA
[c] Johns Hopkins University Applied Physics Laboratory, A1C Structures and Dynamics, Laurel, MD 20723, USA
[d] Applied Research Laboratory, The Pennsylvania State University, State College, PA 16804-0030, USA

ARTICLE INFO

Article history:
Received 31 May 2013
Accepted 17 August 2013
Available online 24 August 2013

Keywords:
Aluminum alloys
Cold-spray coating
Fatigue

ABSTRACT

The effects of cold spray coating and substrate surface preparation on crack initiation under cyclic loading have been studied on Al2024 alloy specimens. Commercially pure (CP) aluminum feedstock powder has been deposited on Al2024-T351 samples using a cold-spray coating technique known as high velocity particle consolidation. Substrate specimens were prepared by surface grit blasting or shot peening prior to coating. The fatigue behavior of both coated and uncoated specimens was then tested under rotating bend conditions at two stress levels, 180 MPa and 210 MPa. Scanning electron microscopy was used to analyze failure surfaces and identify failure mechanisms. The results indicate that the fatigue strength was significantly improved on average, up to 50% at 180 MPa and up to 38% at 210 MPa, by the deposition of the cold-sprayed CP-Al coatings. Coated specimens first prepared by glass bead grit blasting experienced the largest average increase in fatigue life over bare specimens. The results display a strong dependency of the fatigue strength on the surface preparation and cold spray parameters.

1. Introduction

Aluminum usage has become increasingly more commonplace as a means to lighten mechanical components for a wide range of industrial applications. Decreasing product weight by using aluminum alloys rather than steel often comes, however, at the expense of mechanical properties such as wear resistance, surface hardness, and load bearing capacity. Research in this regard has focused on the improvement of aluminum properties by alloying and through the application of coatings deposited by numerous techniques. The overall objective of such work is to achieve coated aluminum alloys with similar or better mechanical performance than that of traditional construction steels, making them effective for an assortment of mechanical applications [1].

Aluminum alloys of the 2xxx series are widely used in aerospace, automotive, and other high performance structural applications due to their high strength-to-weight ratio and low density. Their strength has been increased by the addition of elements such as copper [2]. Such elemental additions also adversely affect the corrosion resistance of the alloy, however, particularly in regard to environments containing halides such as sodium chloride. Consequently, suitable protection treatments such as anodizing, painting, or coating are commonly used on the surface of these high strength aluminum alloys in order to improve their corrosion resistance. Until recently, chromate conversion coatings (CCCs) were the primary choice for a means to protect the surface of high strength aluminum from corrosion, as well as improve its wear resistance [3]. However, hexavalent chromate, Cr(VI), is now recognized as a highly toxic pollutant and its use has been restricted by environmental legislations. Recent research in this area addresses the development of environmentally benign coatings that offer the same corrosion protection as CCCs.

Various potential replacements for chromate conversion coatings, deposited by different coating technologies, have been investigated. The physical vapor deposition (PVD) and chemical vapor deposition (CVD) processes are amongst the more established methods used for the application of such coatings. Many thin hard coatings deposited by PVD and CVD techniques have been shown to enhance the wear and corrosion resistance of mechanical components [1]. PVD methods offer uniform thickness, good control over stoichiometry, relatively low deposition temperature, and the simultaneous coating of the entire object [4]. However, PVD has relatively low deposition rates, and often generates high internal stresses in the hard coatings and poor adhesion to substrates [5]. The advantages of CVD processes are uniform thickness and relatively high deposition rates. However, the high temperatures of the CVD process lead to grain growth, resulting in the loss of enhanced properties associated with small grain-sizes. CVD is also

* Corresponding author. Tel.: +1 5705771754; fax: +1 5705777281.
E-mail address: cziemian@bucknell.edu (C.W. Ziemian).

0261-3069/$ - see front matter © 2013 Elsevier Ltd. All rights reserved.
http://dx.doi.org/10.1016/j.matdes.2013.08.061

relatively difficult to control due to the large number of process variables involved.

While the primary objectives of coating high strength aluminum alloys are typically the improvement of corrosion and wear resistances, the effect of these coatings on other crucial mechanical properties is also of great importance. Fatigue life is one of the most critical design considerations specific to the use of coated 2xxx series aluminum alloys in structural aircraft components [2]. In considering the effect of coatings on component fatigue performance, however, the literature offers contradictory results. Several recent studies have shown that certain coatings enhance the fatigue resistance of coated components [6–10], while others have adverse effects on cyclical loading response. Saini and Gupta [11] found that WC/C PVD coatings increased the endurance limit of case carburized steel by 7% without affecting the hardness or tensile properties. Mcgrann et al. [12] determined that the thermal spraying 6061 aluminum and steel substrates with WC–Co coatings could increase the fatigue life by a factor of ten. The fatigue performance of coated components has also been determined to be dependent on the microstructure, porosity, and mechanical properties of the coatings themselves [13–16]. For instance, Ibrahim and Berndt determined that when WC–Co coatings were applied to AISI 4340 steel by the HVOF process, the major contributor to increased fatigue life was the load carrying capacity of the coatings [13]. Finally, coating adhesion has been shown to affect fatigue performance. While strong coating adhesion is most often a desirable characteristic, Lonyuk et al. [16] determined that it can be detrimental if the mechanical properties of the coating are less desirable than the covered substrate. Their results indicate that when cracks initiate in the coating itself, strong adhesion assists the spread of the cracks into the underlying substrate material, thereby initiating fatigue failure. Consequently, coating brittleness adversely affects fatigue strength as the coating is more susceptible to cracks forming during processing.

In addition to the properties of the coating itself, the surface preparation technique can influence deposition efficiency and bonding between coating and substrate, and the subsequent fatigue performance of the coating–substrate system. For cold spray procedures, it is standard practice to first roughen the substrate surface in order to improve coating adhesion [17]. Cold spray uses a supersonic jet of inert gas in which fine metallic powders particles are injected and accelerated [18]. After achieving a critical velocity specific to the powder and substrate materials, the powders impact the substrate surface with sufficient kinetic energy to plastically deform and mechanically bond to the surface to form a dense coating. The gas stream (typically nitrogen or helium) is heated to approximately 500 °C, at which point it flows through a convergent–divergent (de Laval) nozzle to achieve supersonic speeds [19]. The powder particles are introduced into the gas stream slightly upstream of the converging portion of the nozzle. The highly pressurized and heated gas allows the powder particles to reach velocities up to approximately 1000 m/s. Because the contact time of the spray particles and the pre-heated gas is short, and the gas cools quickly as it expands in the diverging section of the nozzle, the temperature of the powder particles remains far below their melting temperature. Particle temperatures are high enough to improve their ductility and plastic flow upon substrate impact, but they always remain in the solid state, representing the significant difference between cold spray and conventional thermal spray processes [20].

Upon impacting the surface of the substrate, the powder particles mechanically deform via an adiabatic shearing process between the particle/substrate interface and the particle/particle interface [21]. The kinetic energy dispensed during the impact ruptures the surface oxide and plastically deforms the particle as it bonds to the substrate to form a coating [22]. While agreement has yet to be reached on the details of the particle–substrate bonding mechanism, the major advantages of cold spray over thermal deposition techniques clearly result from the fact that the deposition temperatures are low. The elimination of high heat prevents recrystallization from occurring, thereby increasing the probability that the coating will retain the fine grain structure of the initial metallic powder. Unlike conventional thermal spraying processes, cold spray causes almost no oxidation or phase transformation to occur.

The standard surface preparation for the cold-spray process, typically shot peening or grit blasting, involves the bombardment of the substrate with a stream of small hard spherical media, i.e. metal shot or glass beads. This technique is intended to increase the surface roughness of the substrate at the macro-level enough to enhance coating–substrate interaction and to reduce/remove the inherent oxide layer present along an aluminum alloy surface. Shot peening and glass bead grit blasting also impart near-surface compressive residual stresses, which have been shown to reduce the effective applied stresses during service and serve to delay crack initiation and retard early crack propagation on the surface of the bulk material in situations when the coating is properly adhered to the substrate and is free of discontinuities and defects [23]. Asquith et al. [24] demonstrated that mechanical pre-treatment such as shot-peening and grit blasting can increase the fatigue limit 2024-T351 alloy subjected to plasma-electrolytic oxidation (PEO) coating treatment. Secondary observations include the increase in surface microhardness and compressive residual stress profiles, both of which are preferable for mechanical integrity of the coating–substrate system. Similarly, A.L.M. Carvalho and Voorwald [25] studied the beneficial effect of shot-peening on the fatigue resistance of chromium electroplated 7050-T7451 aluminum alloy. Their results demonstrated improved axial fatigue performance associated with glass shot, but decreased axial fatigue strength resulting from ceramic shot. This decrease was attributed to higher surface roughness.

The repeated impacts of shot peening and grit blasting not only induce compressive residual stress, however, but can also refine the microstructure at the surface and sub-surface region and cause damage such as surface dislocations and microcracking [26]. The increased surface roughness and any embedded grit that result from the process can thereby reduce fatigue life, in direct opposition to the increases in fatigue life resulting from the compressive residual stresses imparted on the surface. This has led to contradictory data in the literature regarding the net effect of shot peening and grit blasting processes on the fatigue life of a bulk material. Hatamleh et al. [27] studied the effect of shot peening on friction stir welded 7075-T7351 aluminum plates, and determined that resulting surface morphology can negatively affect the fatigue behavior, thereby hindering some of the gains that result from process-induced compressive residual stresses. Price et al. [28] determined that grit blasting a titanium alloy and applying a pure titanium cold spray coating significantly reduced the fatigue life of the original alloy in rotating bend tests. However, the grit blasting technique has also been shown to increase the fatigue life of thermally sprayed 2024-T3 aluminum alloy by almost 50% [29]. The conflicting results in the literature have been linked to the intensity of the grit blasting and shot peening processes and the associated selection of the process parameters in regard to the subsequent fatigue life of aluminum alloys in rotating bend tests [26]. In order to avoid surface damage and the promotion of crack initiation and growth, shot peening and grit blasting process parameters must be controlled and take into account both the residual stress field and the surface roughness characteristics [23].

The objective of this work is to study the fatigue behavior of 2024-T351 aluminum alloy coated with commercially pure aluminum using the cold-spray process known as high velocity particle

consolidation (HVPC). In this study, the effect of shot peening and glass bead grit blasting surface preparations is analyzed on uncoated 2024-T351 aluminum alloy specimens and specimens that have been additionally cold-sprayed with CP aluminum coatings. All specimens are tested under rotating bending conditions. Subsequent fracture surfaces are examined with a scanning electron microscope (SEM) in order to analyze and identify failure mechanisms.

2. Experimental study

2.1. Materials

The bulk substrate material investigated in this study was 2024-T351 aluminum alloy with the following chemical composition (wt.%): 3.8–4.9 Cu, 1.2–1.8 Mg, 0.3–0.9 Mn, 0.5 Fe, 0.5 Si, 0.25 Zn, 0.15 Ti, 0.1 Cr, and Al balance (90.7–94.7). General mechanical properties of this aluminum alloy are presented in Table 1. The feedstock powder used for the coating was commercially pure (CP) aluminum, which varies from approximately 99.5–99.9% Al. The CP-Al powder used in this study was processed by Valimet Inc. as inert gas atomized with a −325 mesh classification (target mean particle size of 20–35 μm; target overall distribution range of 5–50 μm). Prior to any coating trials, the as-received feedstock powder was analyzed using a scanning electron microcopy equipped with Kevex EDX.

2.2. Substrate preparation

AA2024-T351 test specimens were prepared in several different forms to allow for preliminary coating microstructure and adhesion testing, in addition to the fatigue analysis. Specimens designated for coating microstructure analysis were machined to 25.4 × 25.4 × 6.35 mm squares. Specimens designated for adhesion tests were prepared in two forms. The first form, to be used in pull tests, was a 25.4 mm diameter cylindrical slug with a 38.1 mm length. The second form, to be used in bend tests, was a 25.4 × 152.4 mm specimen with a 2.29 mm thickness. Test specimens designated for the rotating bend fatigue tests were machined from cylindrical AA2024-T351 stock according to the recommendations provided within the published material associated with the Instron R.R. Moore high speed fatigue testing machine [30].

All specimens used for coating microstructure and adhesion analyses, and the portion of the fatigue specimens designated for surface preparation were then shot peened or glass-bead grit blasted. Peened substrates were prepared using an ultrasonic shot peening process and the intensity was measured by the arc height of Almen specimen (A type). The shot media was hard steel balls with 2.0 mm diameter. The shot peening treatment was performed for 5 s per specimen, achieving a peening intensity of 14.5A and 50% coverage. The grit blasting operation applied glass bead (G3) grit with an average particle size of 700 μm diameter, impacting the substrate surface at a 45° angle. The glass bead media is typically less inclined to embed into the substrate surface than other common media, i.e. Al2O3 (alumina) and SiC, due to its lower hardness [31]. In addition, the 45° contact angle was used in an effort to reduce the impact velocity of the grit blast media and decrease the amount of embedded grit, while still producing the desired surface roughness. A schematic of this grit blast operation is illustrated in Fig. 1.

Table 1
Mechanical properties of Al-2024-T351 alloy (substrate material).

Property	Value
Ultimate tensile strength	469 MPa
Tensile yield strength	324 MPa
Modulus of elasticity	73.1 GPa
Ultimate bearing strength	814 MPa
Bearing yield strength	441 MPa
Vickers Hardness	137 HV

Upon completion of surface preparation, the roughness of the substrate surfaces was measured using a Mahr Pocket Surf Portable Surface Roughness Gage contact profilometer in both the longitudinal and transverse directions relative to the substrate. Those specimens designated for cold-spray coating were then cleaned ultrasonically in methyl alcohol and dried using compressed air. Fatigue specimens were further prepared for spraying by taping over the ends to prevent deformation of crucial dimensional and form tolerances required for R.R. Moore rotating bend testing.

2.3. Cold spray coating deposition

Following surface preparation and cleaning, the substrate specimens designated for coating were subjected to a CP-Al coating by cold spray. The cold-spray system used in this study consists of a computer-controlled high-pressure gas delivery system, gas heater, powder feeder, spray gun with a convergent–divergent nozzle to form a supersonic gas jet, sealed-off spraying chamber, and control console. A 200 mm length WC–Co nozzle with a throat diameter of 2 mm, an exit diameter of 7.54 mm, and an expansion length of 168 mm was used to apply the CP-Al coatings. The powder feeder rate was set to 15 ± 5 g/min. Powder particles were accelerated with a nitrogen carrier gas at a temperature of 230 °C and 3.45 MPa pressure. Nitrogen was selected as the carrier gas because it yielded the best results in regard to coating adhesion and subsequent corrosion performance in a related study [31].

The substrates were coated along one axis and stepped at a distance equal to the de Laval nozzle throat diameter (2 mm), using a nozzle traverse speed of 20 mm/s. The entire surface was coated by locating the nozzle in a transverse position a minimum distance of twice the nozzle throat diameter off the edges of the selected substrate. The nozzle–substrate standoff distance for all the spray runs was held constant at 25 mm. The target single-pass coating thickness was 0.152 mm ± 0.075 mm.

2.4. Coating characterization

2.4.1. Coating microstructure and porosity

After the coating was applied, specimens designated for coating microstructure testing were subjected to metallographic examination. This consisted of sectioning the coated specimens perpendicular to the coating traverse, mounting and polishing the specimens using standard metallographic procedures, and analyzing the polished specimens using optical microscopy [31]. Analysis of the optical images included the use of Clemex metallographic evaluation software to determine the percent porosity of the coating.

2.4.2. Coating inspection

Vickers hardness tests were carried out at several sampling points along the coating cross section to account for the variation

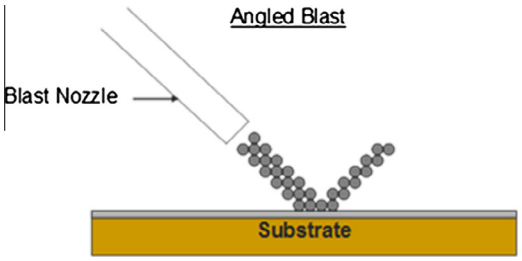

Fig. 1. Schematic of grit blast operation [31].

tendency of hardness across the coating thickness [32]. Individual measurements were done using an applied load of 500 g, and were subsequently averaged. Coating roughness was measured with the Mahr contact profilometer in both the longitudinal and transverse directions. Several coated specimens with each surface preparation were also analyzed on the SEM equipped with energy-dispersive X-ray (EDX) spectroscopy to check composition and ensure that no aluminum oxides formed during the cold-spray process.

2.4.3. Coating adhesion

Cylindrical form specimens underwent adhesion testing as per ASTM: C633-01, "Standard Test Method for Adhesion or Cohesion Strength of Thermal Spray Coatings" to determine the strength of the bond between coating and prepared substrate [31]. One end of each cylindrical slug was coated, with a coating thickness greater than 0.762 mm. The coating was then ground to 0.508 mm to meet the ASTM specification and to create a uniform surface. The coated surface was then bonded to a bare slug using an approved epoxy (Loctite Hysol E214HP). A tensile load was applied to each bonded slug, using a constant crosshead rate of 0.013 mm/s, until rupture occurred and the amount of force required for separation was recorded. Bond strength was determined as the maximum load divided by the cross-sectional area. The coated slugs were examined after failure, and the failure mode was identified per ASTM specification to determine if the coating failed internally (cohesive failure), the coating separated from the slug (adhesive failure), or the coating remained intact and the epoxy failed.

The second type of adhesion tests involved the $25.4 \times 152.4 \times 2.29$ mm rectangular specimens being subjected to guided bend tests per ASTM: E290-13, "Standard Test Method for Bend Testing of Material for Ductility". Three flat plates (with each surface preparation) were first coated to achieve a coating thickness of $0.152 \pm .076$ mm [31]. Coated plates were then bent about a radius and visually inspected to determine if coating cracking or adhesion failure occurred. The plates initially rested freely on two rolling pins and a load was applied to the middle of the plate with a radial component, causing the plate to bend between the rolling pins until a $\sim 180^\circ$ bend was achieved (Fig. 2). The coating surface and edges of the bent portion were then visually examined to determine if coating cracking had occurred.

2.5. Fatigue testing

Fatigue testing of coated specimens was completed as per International Standard ISO 1143, "Metals – Rotating bar bending fatigue testing" [33]. A test matrix that utilized five different treatment types was developed, including bare, shot peened, grit blasted, shot peened and coated, and grit blasted and coated. Ten specimens were processed for each of these specimen types, with five tested at a stress level of 180 MPa and five tested at a stress of 210 MPa. The lower stress level was initially set to be 150 MPa in order to be consistent with other testing on AA2024-T351 substrates in the literature [32], but preliminary tests on bare specimens experienced run-out (defined by 5E7 cycles). In order to ensure fracture and avoid a run-out situation, the lower stress level was adjusted to be 180 MPa.

Each specimen was then subjected to rotating flexural fatigue testing on an Instron R.R. Moore Rotating Bend Fatigue Testing System [30]. Specimens were all rotated at speeds ranging from 7000 to 8500 rpm. Slight variations in rotational speeds were considered acceptable and have been shown to have no significant effect on the ultimate result of R.R. Moore tests [34]. Upon failure, the specimen was removed and the number of cycles-to-failure was recorded. Failed specimens were then machined for subsequent SEM analysis.

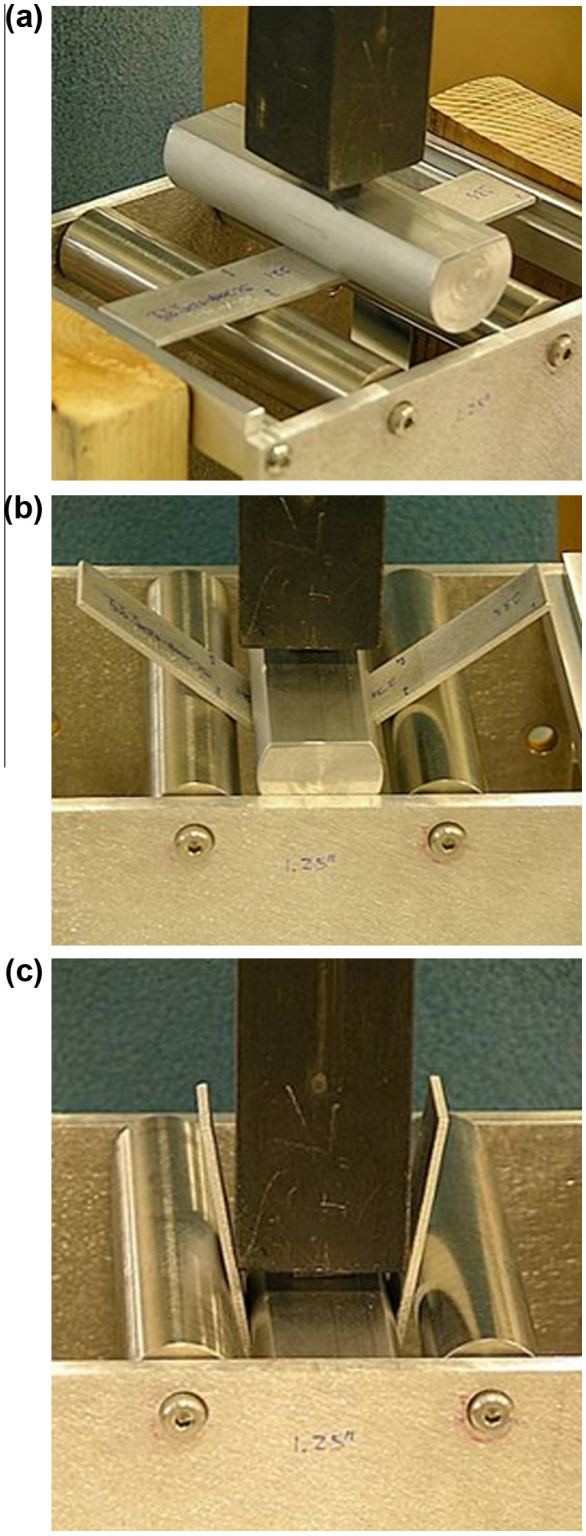

Fig. 2. Guided-bend test apparatus: (a) relaxed state, (b) during loading, and (c) at completion of loading [31].

3. Results and discussion

3.1. Characterization of feedstock powder

Fig. 3(a) shows the SEM results of the morphology analysis of the CP-aluminum feedstock powder, with the majority of the particles exhibiting a spheroidal shape. The results of the particle size

distribution analysis (Fig. 3b) indicate a mean particle diameter of 26.42 μm, with approximately 1.8 vol% below 5 μm and 3.6 vol% above 50 μm. A primary focus was the determination of the volume percentage of particles with diameters smaller than 5 μm, as these smaller particles tend to agglomerate and increase the likelihood of clogging the nozzle [31].

3.2. Characterization of surface-prepared AA2024-T351 substrate

Ten roughness measurements taken from each specimen were averaged to compute the mean values reported in Table 2. Observations of the substrate following shot peening indicated the presence of some minor cracking in some cases.

3.3. Characterization of coating

Using the coating parameters described in Section 2.3, a single-pass coating thickness of 0.127 mm was achieved. The coating composition did not include the formation of any aluminum oxide, as verified by EDX (Fig. 4).

The mean coating thickness applied to the fatigue test specimens was 0.381 mm. Fig. 5 shows an optical micrograph of one of the CP-Al coatings that is representative of those generated during this project [31]. It can be seen that the resulting cold sprayed coatings were dense with some distinguishable micropores, as is typical of such coatings. These pores are the result of the low density of aluminum, as the deformation extent of a particle is generally determined by both its strength and its density [35]. The higher magnification optical micrograph (Fig. 5a) indicates essentially plastically deformed splat morphologies of the CP-Al particles forming the as-sprayed coatings. The particle velocities achieved with the nitrogen carrier gas successfully produced a high degree of powder particle flattening, which also resulted in relatively smooth coating surfaces. Coating roughness measurements were averaged to compute the mean values reported in Table 2.

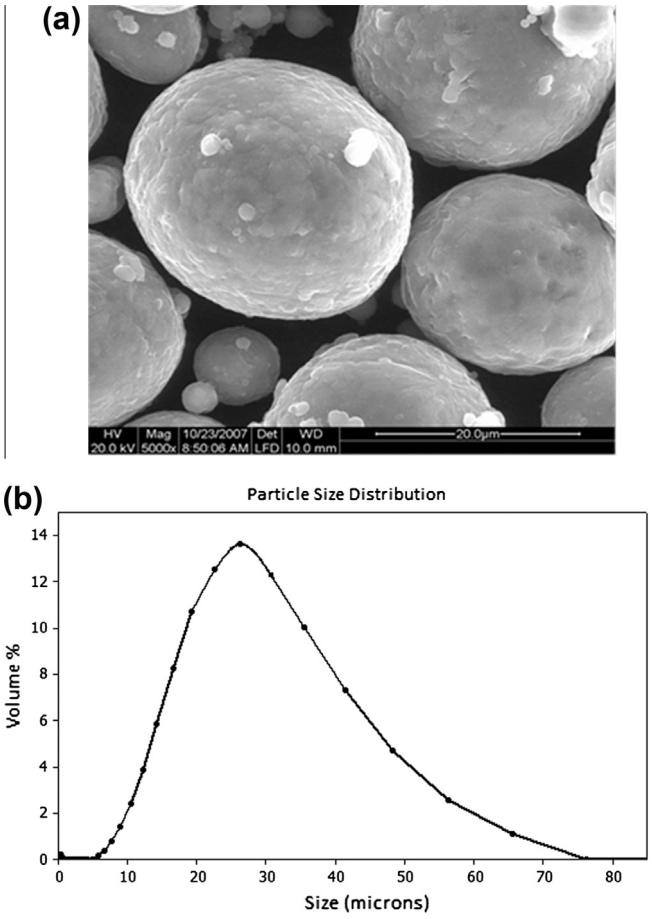

Fig. 3. CP-Al feedstock powder analysis results: (a) SEM surface morphology images at 5000× magnification [31] and (b) particle size distribution.

Fig. 5b shows the coating–substrate interface. Due to the hardness of the AA2024-T3 substrate and the high velocity of the impacting CP-Al powder particles, the local deformation of the CP-Al particles due to particle impact is evident. The general profile of the grit-blasted substrate surface can also be slightly observed, showing its deformation as well. The coating–substrate interface displays very few significant voids, indicating strong adhesion. Bonding between particles and substrate is tight due to the strong deformation of coating and substrate materials.

Coating densities greater than 99% were achieved, with the mean coating porosity determined to be 0.4% (by Clemex Software) for all specimens [31]. The coating porosity was lower for the glass bead blasted specimens, with a range of 0.2–0.5% and a mean value of 0.3%. The specimens that had been shot peened had a coating porosity range of 0.4–0.7% and a mean value of 0.5%. The coating microhardness varied along the coating thickness within the range of 34–70 VHN for all tested specimens. The mean coating hardness for specimens prepared by glass bead grit blasting was 56 VHN.

Coated and bonded slug specimens were subjected to a tensile load using a constant crosshead rate of 0.013 mm/s until rupture occurred, and the amount of force required for separation was recorded. The mean coating/substrate bond strength was determined as the average maximum tensile load divided by the cross-sectional area for five specimens with each surface preparation. The mean coating/substrate bond strength was higher for the glass bead grit blasted specimens than for the shot peened specimens, with a value of 40.65 ± 5.02 MPa. All ten specimens indicated adhesion failures, i.e. the coating separated from the substrate.

In further investigation of coating bond strength, the guided bend tests were completed. Results indicated excellent coating adhesion for the glass bead grit blasted specimens; better than for the shot peened specimens. None of the coating surfaces or edges of the bent portions of the grit blasted specimens displayed any indications of cracking.

3.4. Fatigue performance

The number of cycles-to-failure experienced by each specimen during a rotating bend fatigue test was recorded. Table 3 displays the mean values and the associated standard deviation for each specimen type at the high and low stress levels. Figs. 6 and 7 display the data graphically as interval plots to highlight the variability associated with each specimen type. An increase in rotating bending fatigue strength for AA2024 aluminum alloy was observed as a result of surface treatment followed by CP aluminum coating. The data indicate that the grit blasted/coated specimens performed better than other specimen types at a stress level of 210 MPa, surviving an average of 5.68E+06 cycles to failure. At this stress level, the bare specimens have the smallest fatigue strength, with a mean life of 5.77E+05 cycles to failure. At a stress level of 180 MPa, the mean cycles to failures was again the largest for the grit blasted/coated specimens (1.95E+07), but the shortest fatigue life was associated with the shot-peened/uncoated specimens at 5.38E+06 cycles. The results at this stress level also suffered from a larger amount of variation in the data. A statistical analysis was performed in order to determine the significance of the experimental data.

Results were analyzed as a 2^2-full factorial experiment with two factors (coating and surface preparation) at two levels each (coated/uncoated and shot peened/grit blasted) in order to assess

Table 2
The mean surface roughness of uncoated and coated specimens.

Surface preparation	Average substrate roughness R_A (μm)	Average coating roughness R_A (μm)
None; bare specimen	0.762 (30 μm)	–
Shot peened	1.905 (75 μm)	9.0 (354.3 μm)
Grit blasted	3.302 (130 μm)	8.0 (314.9 μm)

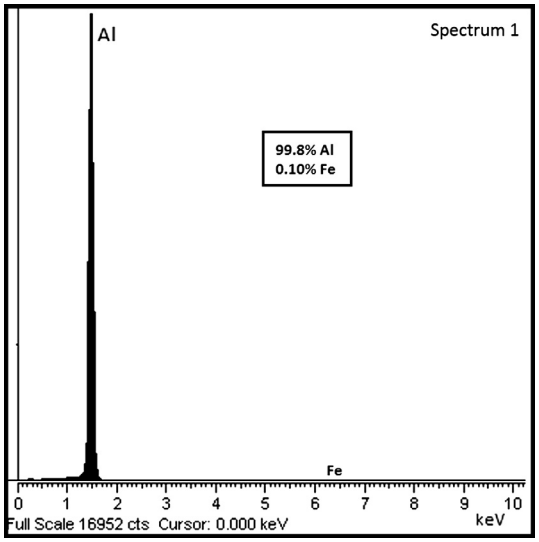

Fig. 4. Energy-dispersive X-ray (EDX) spectrum of a coating on a glass-bead grit blasted substrate.

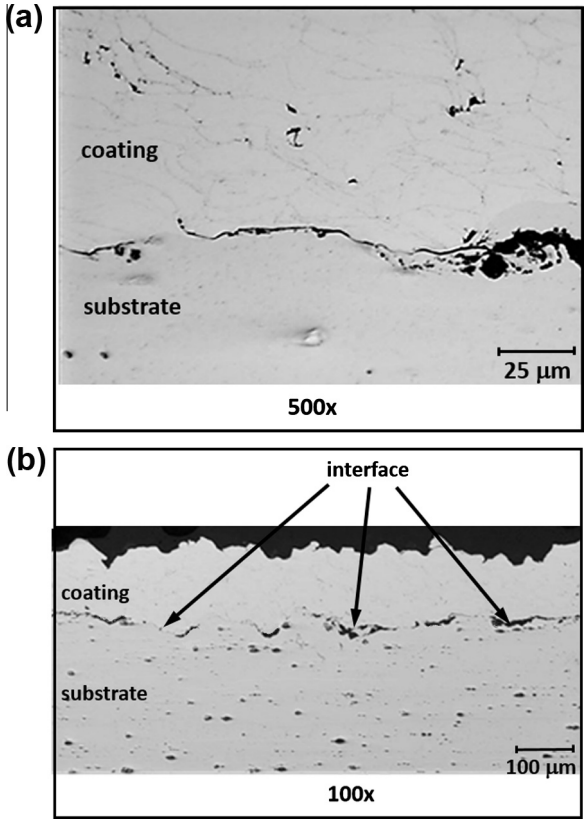

Fig. 5. Optical micrograph of coating microstructure and coating/interface morphology for glass bead grit blasted specimen at magnifications of: (a) 50× and (b) 100×.

the main effects of each factor. The number of cycles to failure was the quantitative response variable measured. To quantify the significance of the CP-Al coating and the surface preparation type, the main factor effects of the experimental factors were computed. The results are presented in Tables 4 and 5.

The data analysis in Table 4 indicates that at a stress level of 180 MPa stress, the coated specimens lasted an average of 4.68E+06 cycles longer than those that had been surface prepared but not coated; an increase of 51%. At a stress level of 210 MPa, the coated specimens lasted an average of 1.23E+06 cycles longer to failure, representing an increase of 38% over specimens that had been surface prepared but not coated. The bare/untreated specimens survived an average of 1.44E+06 cycles to failure at the 180 MPa stress level, with coated specimens lasting 1.39E+07 cycles on average; an increase of 863%. At 210 MPa, the bare/untreated specimens lasted an average of 9.29E+05 cycles to failure, with coated specimens lasting 4.46E+06 cycles on average; an increase of 380%. These results indicate a net increase in the fatigue life of AA2024 specimens resulting from the surface treatment and the CP aluminum cold-sprayed coating. This is further verified by the positive main effect values for coating (Table 4).

The main effects for surface treatment type were also analyzed (Table 5). The average life of the glass bead grit blasted (GB) specimens, and that of the shot-peened (SP) specimens, were determined. The overall mean life of surface treated specimens was also computed. The main effect of glass bead grit blasting was determined as the difference between the mean life of the GB specimens and that of all surface treated specimens. At a stress level of 180 MPa, the grit blasted specimens demonstrated a mean increase in the number of cycles to failure over all surface treated specimens of 4.75E+06 cycles. At a stress level of 210 MPa, this difference was 1.37E+06 cycles. These positive main effect values

Table 3
Mean number of fatigue cycles to failure for each specimen type.

Stress (MPa)	Specimen type	Number of cycles to failure	
		Mean	Std. deviation
180	Bare	9.13E+06	1.34E+06
	Grit Blast (GB)	1.30E+07	4.45E+06
	Peened	5.38E+06	1.55E+06
	GB & coated	1.95E+07	2.97E+06
	Peened & coated	8.17E+06	1.48E+06
210	Bare	5.77E+05	2.79E+05
	Grit Blast (GB)	4.76E+06	6.29E+05
	Peened	1.70E+06	7.25E+05
	GB & coated	5.68E+06	6.63E+05
	Peened & coated	3.23E+06	8.11E+05

indicate the net positive impact on fatigue life of the utilized glass bead blasting in comparison to the shot peening.

Fig. 6 indicates that the shot peened specimens, both coated and uncoated, survived for fewer cycles to failure than the bare or grit blasted specimens at the lower stress level of 180 MPa. The decrease in rotating bend fatigue strength associated with the shot peening process is thought to be primarily due to the surface damage caused by the heavy, large radius shot and the embedded grit that resulted in the substrate surface (Fig. 8). The surface indentations and grit served to form stress raisers on the aluminum alloy substrate during the shot peening process. This mechanism was previously investigated by Mutoh et al. [36], who observed acceleration in the crack initiation process as a result of stress concentrations on a roughened surface, and an associated reduction in fatigue life in peened specimens. The roughening of the surface due to the shot peening process has also been known to cause early

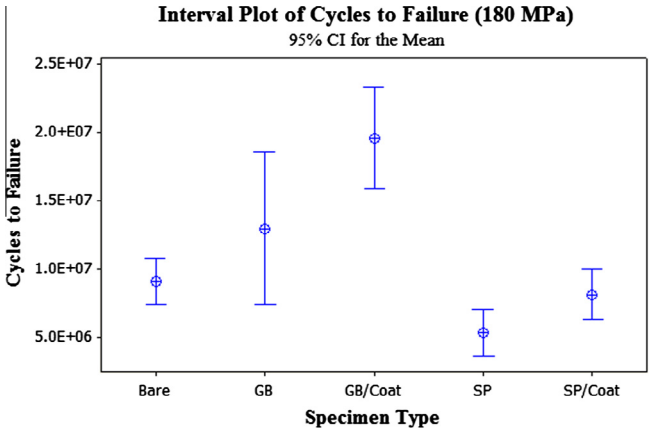

Fig. 6. Fatigue life results at stress level of 180 MPa.

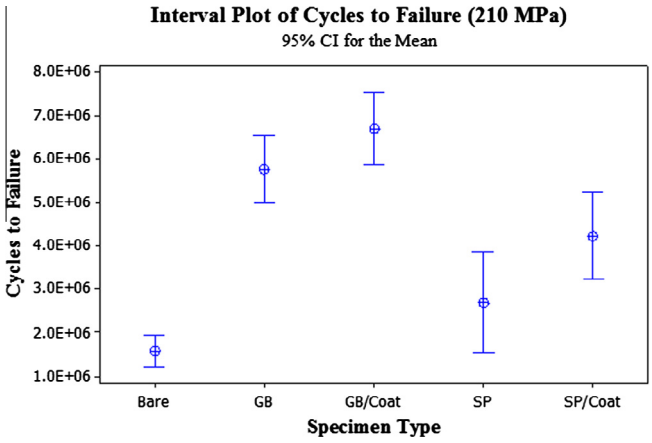

Fig. 7. Fatigue life results at stress level of 210 MPa.

Table 4
Main effects of CP aluminum coating, as compared to uncoated specimens.

Stress (MPa)	Surface Prep	Ave life of specimens:		Main effect of coating
		Coated	Uncoated	
180	Shot Peen (SP)	8.173E+06	5.375E+06	2.340 E+06
	Grit Blast (GB)	1.955E+07	1.299E+07	
	Mean	1.386E+07	9.183E+06	
210	Shot Peen (SP)	3.233E+06	1.704E+06	6.135 E+05
	Grit Blast (GB)	5.680E+06	4.755E+06	
	Mean	4.457E+06	3.230E+06	

Table 5
Main effects of glass bead (GB) surface preparation, as compared to shot peened (SP).

Stress (MPa)	Coated	Ave life of specimens:		Main effect of GB prep
		GB	SP	
180	Yes	1.955E+07	8.173E+06	4.746E+06
	No	1.299E+07	5.375E+06	
	Mean	1.627E+07	6.774E+06	
210	Yes	5.680E+06	3.233E+06	1.374E+06
	No	4.755E+06	1.704E+06	
	Mean	5.217E+06	2.468E+06	

nucleation or the acceleration of fatigue crack propagation in aluminum alloys, as shown by de Camargo et al. [37]. Wagner [38] demonstrated that an increased surface roughness served to accelerate fatigue crack nucleation in aluminum alloys and, consequently, reduced fatigue life. Similarly, Torres [39] observed that stress concentrations on an AISI 4340 steel surface can superimpose with residual stresses formed as a result of shot peening.

In contrast, the results in Table 3 indicate that the average life of the glass-bead grit blasted specimens, both uncoated and coated, is higher than that of the bare specimens at both the high and low stress levels. The lower hardness and smaller diameter (700 μm) of the glass bead media resulted in less surface damage or imbedded grit than shot peening. The results indicate that the grit blast surface preparation is subsequently superior to the utilized shot peening operation in increasing the rotating bend fatigue life of the AA2024-T351 material.

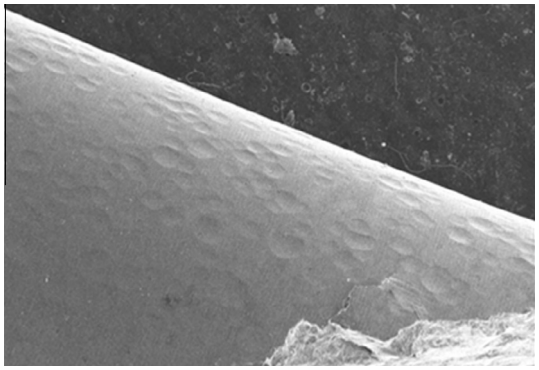

Fig. 8. Substrate surface after shot peening.

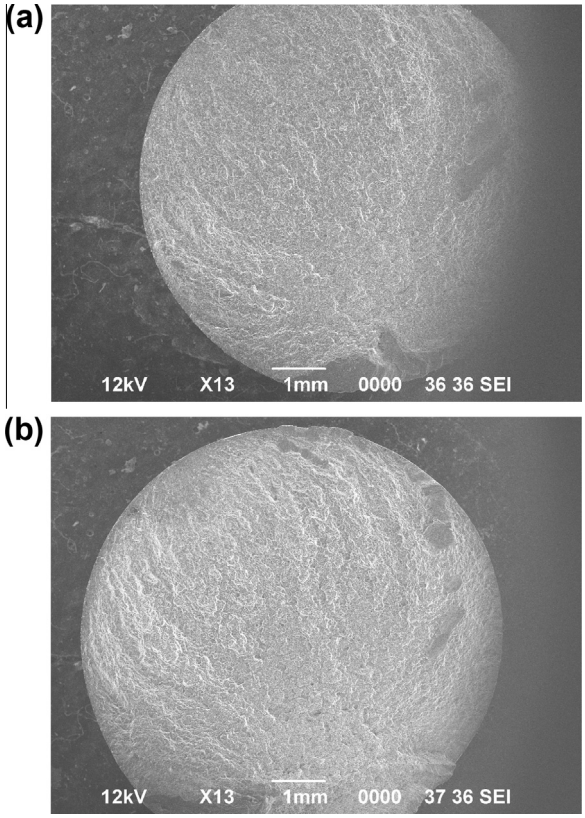

Fig. 9. Crack initiation points on bare specimens at (a) 180 MPa and (b) 210 MPa.

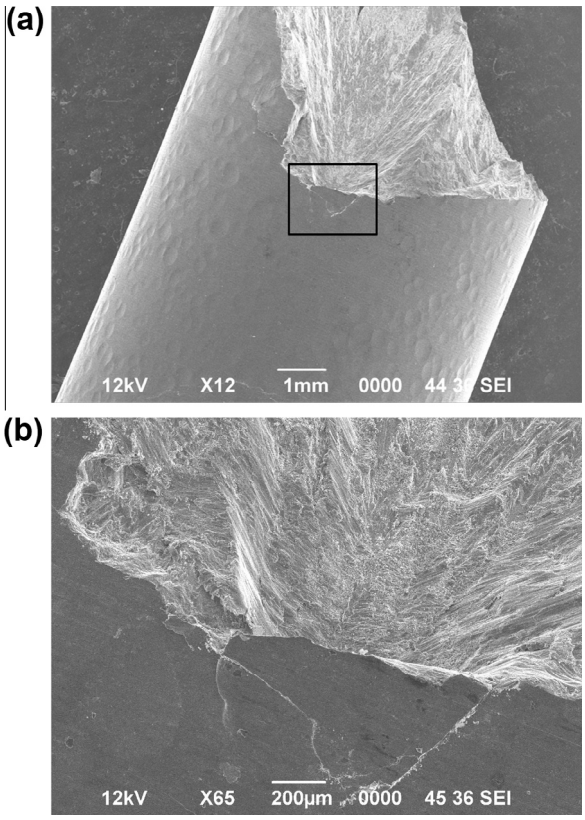

Fig. 10. A representative crack initiation site for an uncoated, shot peened specimen at (a) 12× and (b) 65× magnification.

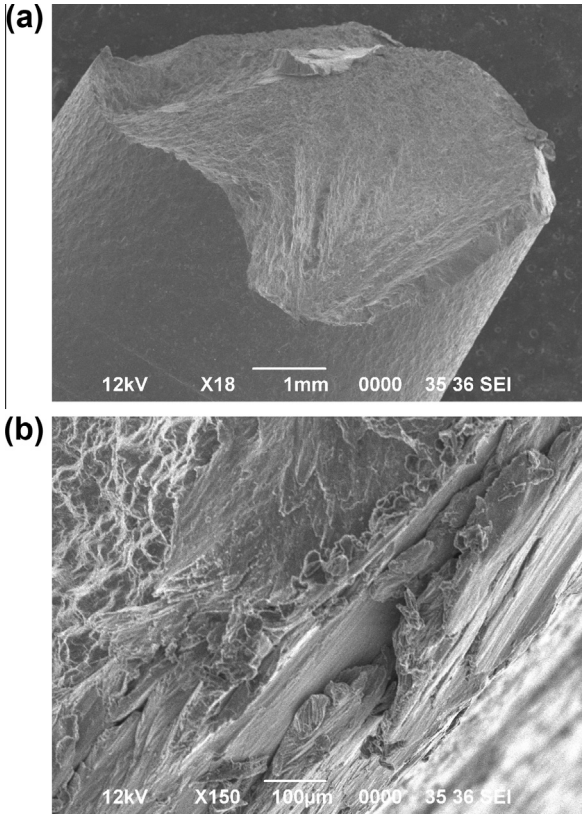

Fig. 11. A representative crack initiation site for an uncoated, grit blasted specimen at (a) 18× and (b) 150× magnification.

3.5. SEM analysis

SEM analysis was performed on the fractured specimens in order to characterize the mechanisms of failure. Analysis of the bare samples revealed that they generally experienced fracture that initiated from flaws on the surface of the specimens at both stress levels, as shown in Fig. 9.

The non-coated specimens, grit blasted and shot peened, displayed similar failure features to the bare untreated substrate, with crack initiation occurring on the surface of the specimens. The initiation points were generally much more pronounced on the surface treated specimens, specifically the shot peened surfaces, than on the bare specimens, as shown in Figs. 10 and 11. This corresponds with the previously discussed finding that the roughening of the specimen surface likely caused stress raisers where failure initiation could originate.

SEM analysis revealed that the shot peened and grit blasted specimens that were subsequently coated with CP aluminum experienced failure that initiated from a variety of sites, not only the surface of specimens like the bare or uncoated surface prepared specimens. The majority of the shot peened/coated specimens tested showed failure that initiated at the substrate/coating interface at both 180 MPa and 210 MPa (Figs. 12–14).

The majority of the grit blast/coated specimens displayed failure that initiated from dimple fracture within the substrate itself. Fig. 15 displays the internal failures of two different specimens that have been grit blasted and coated. Furthermore, these samples revealed adequate coating/substrate adhesion and there were no

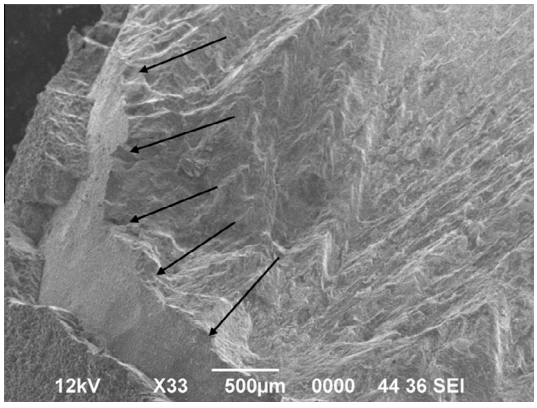

Fig. 12. Substrate/coating interface of shot peened/coated specimen at 210 MPa.

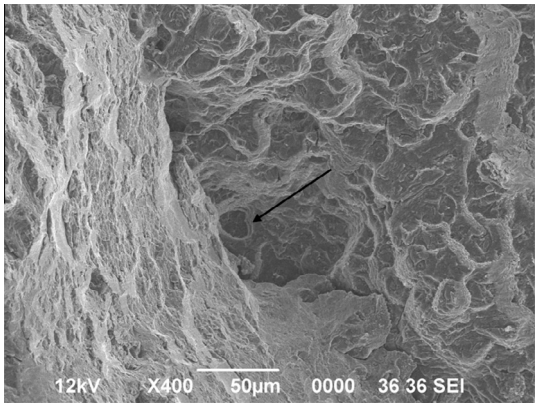

Fig. 13. Pore on the substrate/coating interface of a shot peened/coated specimen at 210 MPa.

inclusions in the initiation sites. This type of failure was revealed in all specimens that experienced improved fatigue life, i.e. a mean fatigue life of 1.30E+07 cycles or greater at 180 MPa, and 4.76E+06 at 210 MPa.

Such failure away from the surface on coated specimens may be assisted by the increase in compressive residual stresses imparted by the cold spray process itself. The process imparts stresses that are highest on the surface of the specimen, and decrease significantly within the bulk of the material [18]. In this situation it is possible for failure to initiate at a point away from the surface of the specimen in the areas of lower residual stresses.

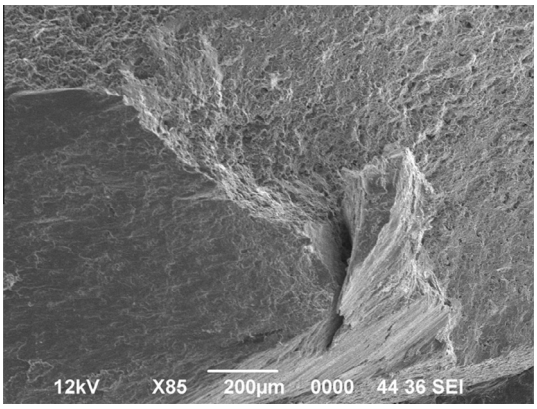

Fig. 14. Failure initiation site on substrate/coating interface of peened/coated specimen at 180 MPa.

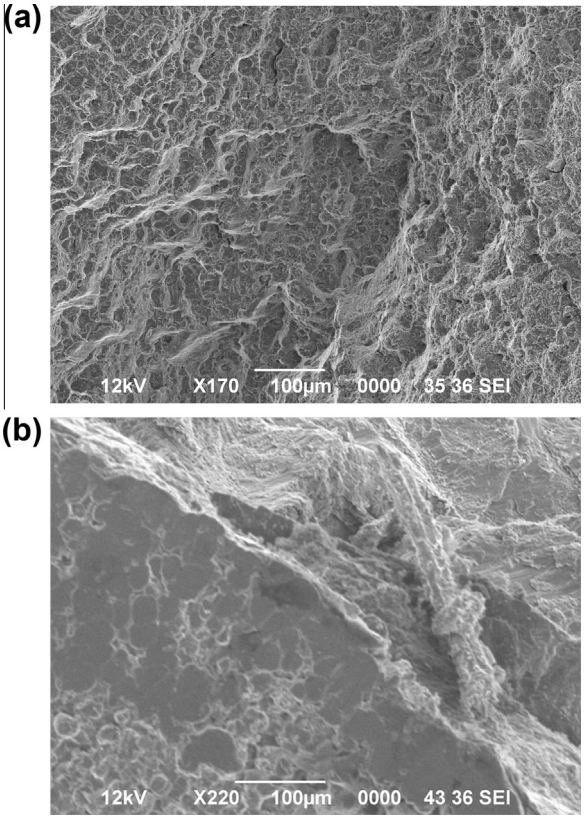

Fig. 15. (a) Dimple and resulting cracks in substrate of grit blast/coated specimen at 180 MPa. (b) Side-view of internal failure site in substrate of grit blast/coated specimen at 210 MPa.

These results indicate that the fatigue initiation sites correspond with a specimen's cycles to failure. In general, crack initiation far from the specimen surface corresponded with a higher number of cycles to failure for the specimen. The bare and shot peened, coated and uncoated, specimens had smaller fatigue lives than the specimens subjected to grit blasting in this study, and most of these specimens failed on the substrate surface or substrate/coating interface. Several of the grit blast/uncoated specimens experienced failure that also initiated at the substrate/coating interface. The grit blast/coated specimens survived for the largest number of average cycles to failure at both stress levels, and showed failure that occurred inside the substrate. These specimens endured more cycles to failure than the bare, peened, peened/coated, or grit blast/coated specimens.

4. Conclusions

The rotating bend fatigue performance of AA2024 specimens was evaluated with varying surface preparations at the stress levels of 180 MPa and 210 MPa. Both uncoated specimens and specimens cold-sprayed with CP-Al were investigated. Data results and specimen analysis indicate the following:

- The 45° glass bead blast surface preparation resulted in higher substrate roughness values, but less surface damage or embedded grit. Coating adhesion was excellent with the 45° glass bead blast surface preparation and superior to that achieved with the more aggressive shot peening process. All coating characteristics were better with the glass bead surface preparation.
- Coating the specimens with CP-Al following a glass-bead blast surface preparation had a significant effect on rotating bend fatigue life, increasing the cycles to failure at both stress levels. At 180 MPa, the fatigue life was increased by 1.04E+07 cycles (110%) on average. At 210 MPa, the fatigue life was increased by 5.10E+06 cycles (850%) on average.
- Increased rotating bend fatigue life is affected by the relative smoothness of the CP-Al coatings which serves to diminish stress raisers on the substrate caused by the surface roughening of the grit blast or shot peening processes.
- At both stress levels, the specimens that were glass bead grit blasted and coated experienced the largest percentage increase in cycles before failure.
- The majority of shot peened/coated specimens at both stress levels experienced failure initiation at sites on the substrate/coating interface and displayed evidence of embedded grit and surface damage.
- The majority of grit blasted/coated specimens experienced fatigue failure initiating from within the substrate. Failure in this manner is likely due to the excessive number of cycles experienced by the specimens prior to failure, with the surface benefited from the compressive residual stresses resulting from surface preparation and coating processes.
- Specimens suffering failure at the surface survived fewer cycles on average than specimens that failed within the substrate.

Additional research is ongoing to more extensively investigate the rotating bend fatigue life associated with glass-bead grit blasted and coated specimens at multiple stress levels, as well as the inherent failure mechanisms, and coating microstructure, residual stresses, and adhesion.

Acknowledgements

The authors acknowledge the Air Force Research Laboratory, Materials & Manufacturing Directorate, Wright-Patterson Air Force

Base, Ohio, USA, for the financial support of this research under Contract No. FA8650-07-C-5214. Any opinions, findings, or recommendations expressed in this paper are those of the authors and do not necessarily reflect the views of the US Air Force.

References

[1] Baragetti S, Lusvarghi L, Bolelli G, Tordini F. Fatigue behaviour of 2011-T6 aluminium alloy coated with PVD WC/C, PA-CVD DLC and PE-CVD SiO_x coatings. Surf Coat Technol 2009;203:3078–87.

[2] Pinc W, Geng S, O'Keefe M, Fahrenholtz W, O'Keefe T. Effects of acid and alkaline based surface preparations on spray deposited cerium based conversion coatings on Al 2024-T3. Appl Surf Sci 2009;255(7):4061–5.

[3] Chen WK, Bai CY, Liu CM, Lin CS, Ger MD. The effect of chromic sulfate concentration and immersion time on the structures and anticorrosive performance of the Cr(III) conversion coatings on aluminum alloys. Appl Surf Sci 2010;256:4924–9.

[4] Malshe AP, Jiang W, Dhamdhere AR. Nanostructured coatings for machining and wear-resistance applications. JOM 2002;54(9):28–30.

[5] Bemporad E, Sebastiani M, Pecchio C, De Rossi S. High thickness Ti/TiN multilayer thin coatings for wear resistant applications. Surf Coat Technol 2006;21(6):2155–65.

[6] Kim KR, Suh CM, Murakami RI, Chung CW. Effect of intrinsic properties of ceramic coatings on fatigue behavior of Cr–Mo–V steels. Surf Coat Technol 2003;171(1):15–23.

[7] Baragetti S, La Vecchia GM, Terranova A. Fatigue behavior and FEM modeling of thin-coated components. Int J Fatigue 2003;25(9-11):1229–38.

[8] Baragetti S, La Vecchia GM, Terranova A. Variables affecting the fatigue resistance of PVD-coated components. Int J Fatigue 2005;27(10–12):1541–50.

[9] Baragetti S. Fatigue resistance of steel and titanium PVD coated spur gears. Int J Fatigue 2007;29(9-11):1893–903.

[10] Gelfi M, La Vecchia GM, Lecis N, Troglio S. Relationship between through-thickness residual stress of CrN–PVD coatings and fatigue nucleation sites. Surf Coat Technol 2005;192(2–3):263–8.

[11] Saini B, Gupta V. Effect of WC/C PVD coating on fatigue behaviour of case carburized SAE8620 steel. Surf Coat Technol 2010;205(2):511–8.

[12] McGrann R, Greving D, Shadley J. The Effect of coating residual stress on the fatigue life of thermal spray-coated steel and aluminum. Surf Coat Technol 1998;108(1-3):59–64.

[13] Ibrahim A, Berndt CC. Fatigue and deformation of HVOF sprayed WC–Co coatings and hard chrome plating. Mater Sci Eng, A 2007;456(1-2):114–9.

[14] Oh J, Komotori J, Song J. Fatigue strength and fracture mechanism of different post-fused thermal spray-coated steels with a co-based self-fluxing alloy coating. Int J Fatigue 2008;30(8):1441–7.

[15] Akebono H, Komotori J, Shimizu M. Effect of coating microstructure on the fatigue properties of steel thermally sprayed with Ni-based self-fluxing alloy. Int J Fatigue 2008;30(5):814–21.

[16] Lonyuk B, Apachitei I, Duszczyk J. The effect of oxide coatings on fatigue properties of 7475-T6 aluminium alloy. Surf Coat Technol 2007;201(21):8688–94.

[17] Ghelichi R, Guagliano M. Coating by the cold spray process: a state of the art. Frattura Ed Integrità Strutturale 2009;8:30–44.

[18] Alknimov AP, Kosarev VF, Apayrin AN. Cold gas dynamic spray method for applying a coating. US Patent 5, 302, 414, April 12, 1994.

[19] Grujicic M, Zhao C, DeRosset W, Helfritch D. Adiabatic shear instability based mechanism for particles/substrate bonding in the cold-gas dynamic-spray process. Mater Des 2004;25(8):681–8.

[20] Ajdelsztajn L, Jodoin B, Kim G, Schoenung J. Cold spray deposition of nanocrystalline aluminium alloys. Metall Mater Trans A 2005;36(3):657–67.

[21] Assadi H, Gartner F, Stoltenhoff T, Kreye H. Bonding mechanism in cold gas spraying. Acta Mater 2003;51:4379–94.

[22] Dykhuizen RC, Smith MF, Gilmorew DL, Neiser RA, Jiang X, Sampath S. Impact of high velocity cold spray particles. J Therm Spray Technol 1999;8/4:559.

[23] Turski M, Clitheroe S, Evans AD, Rodopoulos C, Hughes DJ, Withers PJ. Engineering the residual stress state and microstructure of stainless steel with mechanical surface treatments. Appl Phys A Mater Sci Process 2010;99:549–56.

[24] Asquith DT, Yerokhin AL, Yates JR, Matthews A. Effect of combined shot-peening and PEO treatment on fatigue life of 2024 Al alloy. Thin Solid Films 2006;515(3):1187–91.

[25] Carvalho ALM, Voorwald HJC. Influence of shot peening and hard chromium electroplating on the fatigue strength of 7050-T7451 aluminium alloy. Int J Fatigue 2007;29(7):1282–91.

[26] Evans A, Bruno G. Relaxation of residual stress in shot peened Udimet 720Li under high temperature isothermal fatigue. Int J Fatigue 2005;27:1530–4.

[27] Hatamleh O, Lyons J, Forman R. Laser and shot peening effects on fatigue crack growth in friction stir welded 7075-T7351 aluminum alloy joints. Int J Fatigue 2007;29:421–34.

[28] Price T, Shipway P, McCartney D. Effect of cold spray deposition of a titanium coating on fatigue behavior of a titanium alloy. J Therm Spray Technol 2006;15(4):507–12.

[29] Sharp PK, Barter SA, Baburamani P, Clark G. Fatigue life recovery in aluminium alloy aircraft structure. Fatigue Fract Eng Mater Struct 2002;25(2):99–109.

[30] Instron Industrial Products. R.R. Moore rotating beam fatigue testing system. POD_RRMoore_rev7_0210. <http://www.instron.us>; 2010

[31] Golesich B, Eden T, Potter J, Wolfe D, Norris A, Sharma M. Innovative corrosion protection via cold spray/kinetic metallization. API Defense, Inc., Engineering Division. Report number AFRL-RX-WP-TR-2010-4022; 2010.

[32] Li W, Huang C, Yu M, Liao H. Investigation on mechanical property of annealed copper particles and cold-sprayed copper coating by a micro-indentation testing. Mater Des 2013;46:219–26.

[33] ISO 1143:2010. Metallic materials – rotating bar bending fatigue testing. International Organization for Standardization; 2010.

[34] Kaufman JG. Properties of aluminium alloys: tensile, creep, and fatigue data at high and low temperatures. ASM International; 1999.

[35] Li W, Zhang C, Guo X, Zhang G, Liao H, Li C, et al. Effect of standoff distance on coating deposition characteristics in cold spraying. Mater Des 2008;29:297–304.

[36] Mutoh Y, Fair GH, Noble B, Waterhouse RB. The effect of residual stresses induced by shot-peening on fatigue crack propagation in two high strength aluminum alloys. Fatigue Fract Eng Mater Struct 1987;10(4):216–72.

[37] de Camargo JA, Cornelis HJ, Cioffi VMO. Coating residual stress effects on fatigue performance of 7050-T7451 aluminium alloy. Surf Coat Technol 2007;201(24):9448–55.

[38] Wagner L. Mechanical surface treatments on titanium, aluminum and magnesium alloys. Mater Sci Eng A 1999;23:210–6.

[39] Torres MAS. An evaluation of shot peening effect in the fatigue life of AISI 4340 steel with and without hard chromium plating. Doctoral Thesis, State University of Sao Paulo, Brazil; 2002.